Preparation of Sialons by the Nitrided Pressureless Sintering (NPS) Technique

I. W. M. Brown

Chemistry Division, DSIR, Lower Hutt, New Zealand

R. Pompe & R. Carlsson

Swedish Ceramic Institute, Göteborg, Sweden

Abstract

The nitrided pressureless sintering (NPS) technique has been used to prepare sialon compositions in the $O'-\beta'$ field, along the $Si_3N_4-Al_2O_3$ join. Samples were fully nitrided in less than 4 h at 1370°C, conditional upon achieving sufficiently high surface areas during milling. TGA and XRD analyses indicate that the nitridation mechanism involves the early formation of yttrium silicate phases during the prenitridation step which are in turn consumed below the nitridation temperature, probably in favour of a partial $Si_3N_4-SiO_2-Y_2O_3-Al_2O_3$ liquid phase. Yttrium aluminium garnet (YAG), whose volume fraction increases with time at temperature and with increasing level of Al addition, is formed promptly under these nitridation conditions. Sintering of the fully nitrided materials in nitrogen was carried out in the temperature range 1500–1830°C, with specimens achieving maximum density by 1600°C. XRD analysis reveals that the sole product of sintering low alumina compositions was β'-sialon.

Sialon Zusammensetzungen im $O'-\beta'$ Feld wurden entlang der $Si_3N_4-Al_2O_3$ Grenze durch druckloses Sintern mit paralleler Nitridierung (NPS) hergestellt. Die Proben konnten nach dem Mahlen zur Erzeugung ausreichender spezifischer Oberflächen bei 1370°C in weniger als 4 h vollkommen nitridiert werden. TGA- und XRD-Messungen zeigten, daß vor der Nitridierung frühzeitig die Bildung von Yttrium-Silikat-Phasen stattfand, die ihrerseits noch unterhalb der Nitridierungstemperatur wahrscheinlich zugunsten

einer $Si_3N_4-SiO_2-Y_2O_3-Al_2O_3$ Flüssigphase aufgebraucht wurden. Yttrium-Aluminium-Granat (YAG), dessen Volumenanteil sich mit der Zeit, der Temperatur und zunehmender Al-Zugabe erhöhte, bildete sich unter den Nitridierbedingungen umgehend. Das vollständig nitridierte Pulver wurde in Stickstoff im Temperaturbereich 1500–1830°C gesintert, wobei die bei 1600°C gesinterten Proben die höchste Dichte erreichten. XRD-Messungen zeigten, daß Zusammensetzungen mit wenig Al_2O_3 reines β'-Sialon als Endprodukt ergaben.

On a préparé des SiAlONs dans la zone $O'-\beta'$ le long de la ligne $Si_3N_4-Al_2O_3$ par frittage naturel nitrurant (NPS). Les échantillons ont été totalement nitrurés en moins de 4 h à 1370°C lorsque la surface spécifique obtenue par broyage est suffisamment élevée. Les analyses par ATG et par diffraction X indiquent que le mécanisme de nitruration met en jeu la formation préliminaire de silicates d'yttrium lors de l'étape de prénitruration, qui sont ensuite consommés à une température inférieure à la température de nitruration, probablement au profit d'une phase liquide partielle du système $Si_3N_4-SiO_2-Y_2O_3-Al_2O_3$. Le grenat d'yttrium et d'aluminium (YAG), dont la fraction volumique augmente lorsque l'on maintient le matériau en température ou que l'on augmente la teneur en Al, se forme rapidement dans ces conditions de nitruration. On a fritté les matériaux totalement nitrurés dans l'azote entre 1500 et 1830°C, avec un maximum de densité à 1600°C. La diffraction X indique que l'unique produit du frittage des compositions pauvres en alumine est le SiAlON β.

1 Introduction

Sialon ceramics are used increasingly in material applications where the properties of strength, hardness, abrasion resistance and thermal shock resistance are important. Although sialons are the focus of many engine component development programmes, the principal commercial applications of sialons to date are in cutting tool technology. In applications where high temperature creep resistance is important, the levels of sintering aids may need to be very low so as to avoid excessive intergranular glassy phase formation. Alternatively, the glassy phase composition needs to be designed so that it can be crystallised to more refractory, creep-resistant phases upon further heat treatment. One conventional approach is to wet mill appropriate proportions of Si_3N_4, AlN and Al_2O_3, usually with Y_2O_3 as a sintering aid. This is followed by drying, pressing (usually CIP) and sintering at temperatures of the order of 1800°C. Submicron-sized Si_3N_4, AlN and Y_2O_3 are relatively expensive raw materials and add substantially to the processing costs which escalate further when high processing temperatures are involved. The compromise of increased sintering aids versus lower processing temperatures may not be suitable for achieving the desired materials properties. Processing techniques such as those described in this paper offer an important alternative technology which can circumvent or reduce some of the difficulties and costs associated with conventional sialon processing.

The nitrided pressureless sintering (NPS) technique has been developed by Pompe and co-workers[1-3] to assist the densification of Si_3N_4-based materials. The principal characteristics of the technique are to use mixed $Si:Si_3N_4$ powders, typically of mass ratio 5:5–7:3, which are milled to achieve submicron particle size. The substitution of Si for much of the Si_3N_4 offers substantial savings in raw material costs. The role of the added Si_3N_4 is two-fold: it acts as a dispersing agent to reduce agglomeration of fine Si particles during milling and helps maintain reaction control by modifying the pore structure during nitridation and by moderating the effect of the exothermic nitridation reaction. Typically, Y_2O_3 (6 %wt with respect to the nitrided Si_3N_4) and Al_2O_3 (2 %wt) are added as sintering aids. Si_3N_4 bodies prepared by the NPS technique are characterised by high green densities (typically 70% or higher after nitridation), narrow pore size distribution, fast nitridation times (2–4 h) and relatively low firing shrinkage ($\approx 10\%$), when compared to other techniques of reaction bonding

or pressureless sintering. A further advantage is the option of machining after the nitridation step, prior to sintering.

This study has been undertaken to demonstrate the earlier-described[2] applicability of the NPS technique to sialon compositions, with particular emphasis on the low alumina end of the Si_3N_4–Al_2O_3 join. By choosing this composition region the processing can be simplified by eliminating AlN from the sialon raw material components. Conventionally, AlN additions are required to achieve monophase β'-sialon,[4] but in the present case we propose to examine the region of the sialon behaviour diagram along the Si_3N_4–Al_2O_3 join as it offers the opportunity to achieve mixed O'–β' sialon microstructure with the inherent properties of improved oxidation resistance due to the O' phase (Si_2N_2O) and high strength due to the β'-phase.[5] Previous workers[6] have reported structural studies of β'-sialon prepared directly from two-component mixtures of Si_3N_4 and Al_2O_3. The combination of high green density, narrow pore size distribution and fine particle size featured by this technique is anticipated to enhance the sinterability of sialons resulting in materials of fine-grained microstructure and improved mechanical properties. The present paper reports the process chemistry relating to the nitridation and sintering of sialon bodies prepared by the NPS technique, and expands and extends our previous work on this subject.[7] The microstructural examination of NPS sialons will be reported elsewhere.

2 Experimental

2.1 Compositions

Four sialon compositions were prepared (called here compositions 1–4) having 15·7, 19·7, 29·7 and 36·2 %wt Al_2O_3, respectively. The location of these compositions on the sialon behaviour diagram is illustrated in Fig. 1. Previous authors[5,8,9] have presented widely varying data for the solubility limit of aluminium in O'-sialon and the present choice of compositions accommodates the two most extreme values reported for aluminium solubility. Compositions 1 and 2 represent points on the behaviour diagram where the proposed O'–β' tie-lines of Thompson *et al.*[5] and Jack[8] intersect with the Al_2O_3–Si_3N_4 join. Compositions 3 and 4 lie outside the region enclosed by the O'–β' tie-lines and may more appropriately be described as lying in the β'-X-phase region. In all compositions 75% of the required Si_3N_4 was added as Si, consistent with
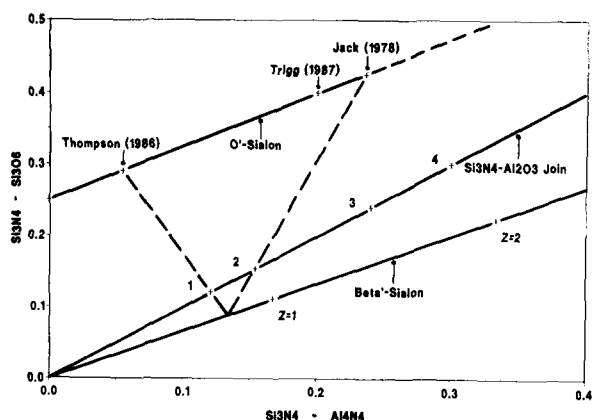
Fig. 1. Composition points on the sialon behaviour diagram.

previous applications of the NPS technique.[1-3] Further, 6 %wt Y_2O_3 (with respect to the nitrided composition) was added as a sintering aid. It must be acknowledged that the added Y_2O_3 may well play a role in modifying the aluminium solubility in the sialons and therefore the exact location of the $O'-\beta'$ tie-lines, as they relate to the present compositions, may vary from the 2-dimensional display in Fig. 1. An additional preparation of composition 2 with 3% added Y_2O_3 (half the standard addition) was carried out to help clarify the role of this additive in the nitridation chemistry and densification processes.

2.2 Powder preparation and fabrication of test specimens

The commercial powders used for the NPS sialon preparation are shown in Table 1, with their measured BET specific surface areas as indicated. The powders were prepared as 150 g batches, transferred to polythene bottles and milled for up to 96 h in *n*-butanol using spherical Si_3N_4 milling media. A sample (3 %wt) of oleic acid was added as a pressing aid. After milling, the butanol slurry was wet-filtered through 10 μm cloth followed by careful rotary evaporation. Residual butanol (2–4 %wt) was left in the powder to assist the oleic acid pressing aid. The powders were granulated through a 500 μm sieve then pre-pressed in an acrylic mould to form 10 g test bars of approximate dimensions 70 × 15 ×

Table 1. Powders used for NPS sialon preparation

Powder source		BET specific surface area $(m^2 g^{-1})$
Si	KemaNord Sicomill 2D	1·9
Si_3N_4	HC Starck LC10	11·9
Al_2O_3	Sumitomo AKP50	9·4
Y_2O_3	HC Starck 'Fine'	16·2

Table 2. BET surface areas of milled powders for NPS sialon preparation

Composition	A series $(m^2 g^{-1})$	B series $(m^2 g^{-1})$
1	9·5	20·2
2	12·4	22·9
3	11·1	21·1
4	11·6	20·6

8 mm before being CIPped at 350 MPa. Finally, the remaining organics were removed using the rate controlled extraction (RCE) technique[10] at temperatures up to 500°C. Two series of the four compositions were prepared, namely series A and series B, having mid-range and high surface areas, respectively. Table 2 shows the measured BET surface areas for series A and B samples. The green densities for series A samples lie in the range 62–65% theoretical, whereas the series B samples lie in the range 57–60% theoretical.

2.3 Nitridation technique

The initial nitridation conditions were defined using TGA techniques on test pieces of mass 1·2–1·5 g using a Mettler TA1 thermobalance (Mettler, Zurich, Switzerland). The samples were placed in an alumina crucible and the balance system was evacuated and flushed twice with nitrogen (AGA 'Plus' grade: <5 ppm O_2, <5 ppm H_2O). Samples were heated at 15°C min^{-1} to 1200°C for 60 min as a pre-nitridation step, then at 4°C min^{-1} to the chosen nitridation temperature, followed by soaking at temperature until no further weight gain took place.

Test bars were nitrided in a Balzers graphite resistance furnace following a heating scheme similar to that described above. The test bars were placed on a silicon nitride powder bed in a graphite box (20 × 20 × 30 cm) and were heated for defined times at 1370°C. Changes in density, linear shrinkage, mass and phase composition (by XRD) were used to monitor the progress of the nitridation reaction, including the effect of the pre-nitridation step. Dilatometric analyses (TDA) were undertaken using a Harrop TD-716 instrument (Harrop, Columbus, OH) operating at 5°C min^{-1} in a nitrogen atmosphere. The instrument was evacuated and flushed twice with nitrogen prior to the commencement of the experiments.

2.4 Sintering technique

Test bars for sintering were packed in an Si_3N_4 powder bed in a graphite box before firing in a Balzers graphite resistance furnace. A small quantity of fine silica powder was added to the powder bed to

provide SiO in the sintering atmosphere. The furnace was evacuated and refilled twice with nitrogen prior to heating at 20°C min^{-1} to 800°C. At this temperature the furnace was fully evacuated to below 10^{-5} bar for 3 h, refilled with nitrogen and the heating program resumed at 20°C min^{-1} until the desired sintering temperature was achieved. Specimens of compositions 1A–4A and 1B were sintered for 3 h at a range of temperatures between 1500°C and 1830°C. The degree of sintering was monitored by measurements of density and porosity (by water intrusion under vacuum), linear shrinkage, weight loss and phase composition changes (by XRD).

3 Results and Discussion

3.1 Nitridation chemistry

Figure 2(a) shows a typical TGA curve for a specimen of composition 1B cut from a larger test bar. The heating schedule contains a pre-nitridation step at 1200°C for 1 h and the results may be compared with Fig. 2(b) in which the pre-nitridation
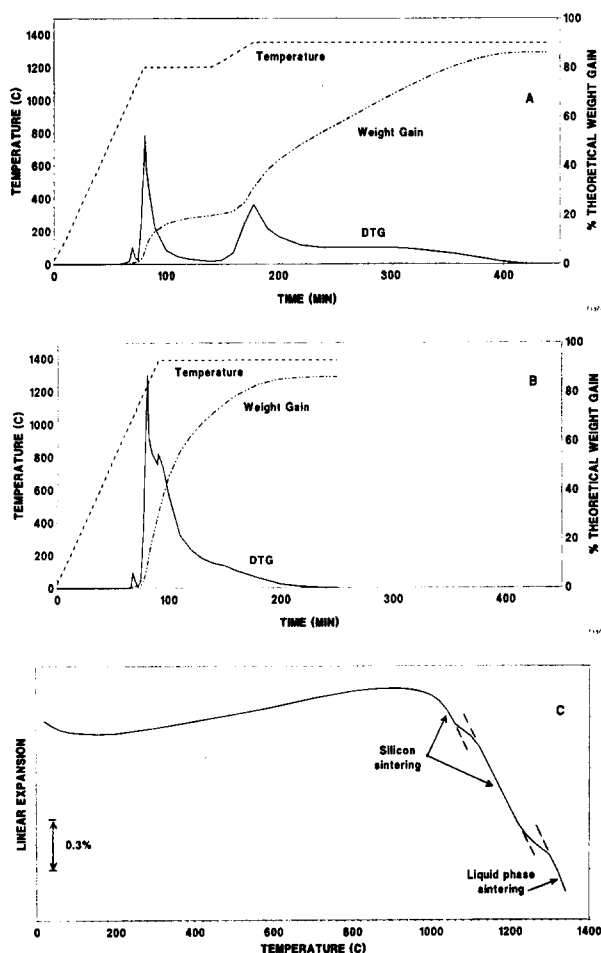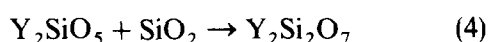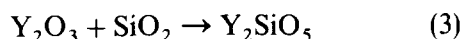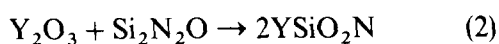

Fig. 2. TGA and TDA curves for NPS sialon nitridation. (a) TGA (1B) including pre-nitridation step; (b) TGA (1B) excluding pre-nitridation step; (c) TDA (2B) excluding pre-nitridation step.

step is omitted from the heating schedule. The onset temperature for nitridation is 1150°C but in each experiment a small weight gain (0·25%) could be observed immediately prior to the commencement of the main nitridation reaction. This preliminary reaction is accompanied by a discrete DTG peak commencing at 1010°C and centred at 1050°C. The origin of this early reaction is unclear as the amount of material formed is small and precludes any opportunity for XRD identification. Nevertheless, two possible explanations may be proposed:

(i)   fast, early nitridation of an extremely fine fraction of silicon powder, or

(ii) reaction of some surface silica on the silicon grains to form a small quantity of Si_2N_2O, according to the reaction:

$$SiO_2 + 3Si + N_2 \rightarrow 2Si_2N_2O \qquad (1)$$
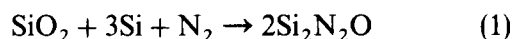
An initial nitridation step prior to the main nitridation reaction has been reported previously for studies of silicon powder reactivity towards nitrogen.[11] In that study the silicon powder was substantially more coarse than in the present experiments and the compositions did not include Y_2O_3, leading to reported commencement of nitridation some 150–200°C higher than in the present experiments. The initial nitridation step was described[11] as the formation of a surface layer of polycrystalline Si_3N_4 on the silicon surface, replacing the original SiO_2 layer. In the present case, the much reduced reaction temperature may be due to the high powder surface area and the presence of Y_2O_3.

In Fig. 2(b), where the reaction temperature has been allowed to rise continuously to the chosen nitridation temperature, the DTG curve shows a maximum nitridation rate at 1240°C. In Fig. 2(a), there is obvious interruption to the nitridation process at the 1200°C pre-nitridation temperature, demonstrating the improved process control of the exothermic nitridation reaction that can be achieved by simple manipulation of the nitridation schedule. Figure 2(c) shows a TDA curve for the nitridation of composition 2B. The first substantial linear shrinkage occurs just above 1000°C. Comparison of the TDA curve with the DTG data in Fig. 2(b) shows that the first DTG peak also commences at this temperature. Further, there is an inflexion in the TDA curve at 1060°C which is coincident with the top of this early DTG peak, i.e. both the TDA and DTG show a slowing down of the reaction processes at this point. Three simultaneous events may be active during this early phase of weight gain and shrinkage: first, Y_2O_3 may react with surface silicon

oxide to form yttrium silicates such as those proposed in reaction schemes (2)–(4), thereby exposing clean silicon surfaces; secondly, the silicon has a strong tendency to sinter, contributing significantly to the early shrinkage; thirdly, the exposed silicon surface will begin to nitride by either or both of the mechanisms (i) and (ii), above. The TDA curve then shows an increase in the shrinkage rate above 1110°C with a further inflexion at 1230–1240°C. Once again this is coincident with the DTG maximum at 1240°C. The nitridation rate proceeds at its fastest during this temperature interval and is characterised by a period of continuous shrinkage, which is most probably due to continued silicon sintering behaviour.[3] Si_3N_4 does not wet silicon and thus will tend to minimise its surface area, leaving exposed silicon surfaces. These may persist up to the point indicated by the DTG maximum and the inflexion in the shrinkage behaviour at 1240°C, when it may be assumed that there will be substantial cover of the silicon surface. At 1300°C the TDA curve shows accelerating shrinkage which is consistent with the formation temperature of the first liquid phase in this system.[12]

The pre-nitridation step in NPS processing (1200°C for 60 min) is accompanied by early reaction of all Y_2O_3. One of the principal functions of this sintering aid is to react with the small quantity of silicon oxide and oxynitride[13] associated with the Si and Si_3N_4, thus exposing fresh Si surfaces to nitrogen. XRD data for all major phases in the nitridation chemistry are shown in Fig. 3. In series A samples (low surface areas) the Y_2O_3 is converted to poorly crystallised Y_2SiO_5, $YSiO_2N$ (YN-wollastonite) and α-$Y_2Si_2O_7$. In the higher surface area series B samples better crystallised α-$Y_2Si_2O_7$ becomes the dominant phase upon pre-nitridation. It is likely that the chemistry of the nitridation process follows the same mechanism in both series, but is more accelerated in the higher surface area series B samples. These products are consistent with the following reaction schemes:

$$Y_2O_3 + Si_2N_2O \rightarrow 2YSiO_2N \qquad (2)$$

$$Y_2O_3 + SiO_2 \rightarrow Y_2SiO_5 \qquad (3)$$

$$Y_2SiO_5 + SiO_2 \rightarrow Y_2Si_2O_7 \qquad (4)$$

Series A samples showed 10–12% conversion of Si to Si_3N_4 on pre-nitridation, whereas for the series B samples, 14–16% conversion was achieved. All samples displayed per cent conversion values directly proportional to their powder surface areas (see Table 1). The role of this pre-nitridation step is to nucleate the nitride as well as to maintain process
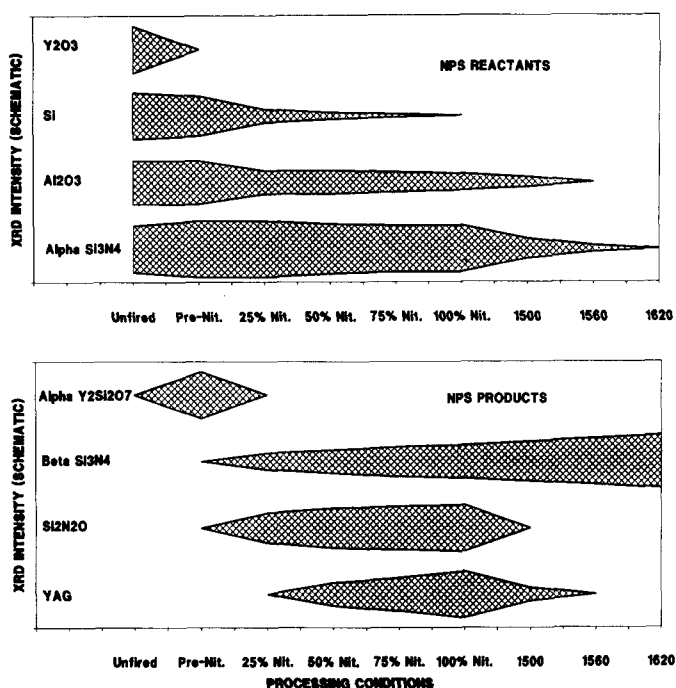

Fig. 3. Phase development during NPS sialon nitridation: effect of temperature.

control during the initial stages of the exothermic nitridation reaction.

Figure 4 shows the dependence of nitridation rate on powder surface area for the two series of four compositions nitrided at 1350°C in a thermobalance. It is clear that a surface area above 13–14 m² g⁻¹ is required to reduce the nitridation time to below 4 h. Under these conditions, powder surface areas and nitridation times are similar to those observed in studies of NPS Si_3N_4 formation.[1]

The effect of temperature on nitridation rate for composition 1B has been measured at 20°C intervals between 1330°C and 1410°C. Figure 5 shows that there is a linear reduction in nitridation time between 1330°C and 1410°C with extremely fast
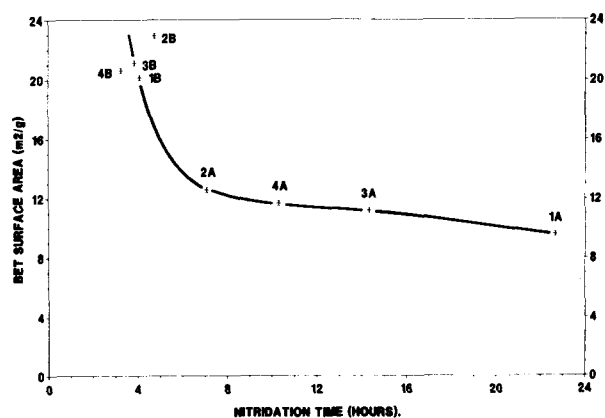

Fig. 4. Dependence of nitridation rate on powder surface area for NPS sialon compositions.
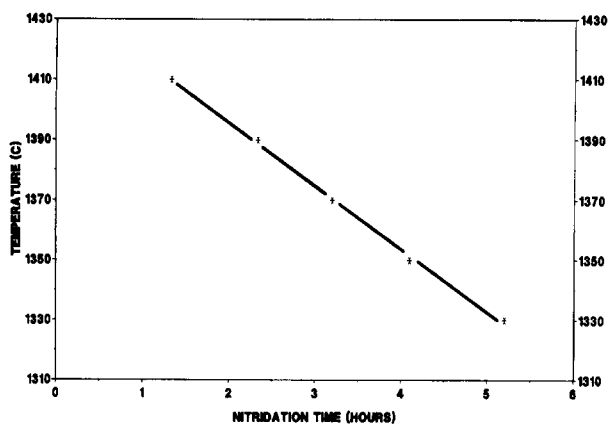
Fig. 5. Dependence of nitridation rate on temperature for NPS sialon composition 1B.

nitridation being achieved at the highest temperature. However, it should be noted that this temperature is very close to the melting point of the silicon powder, given the additional factor of the exothermic nature of the nitridation reaction. Further, we have shown that partial liquid phase formation in the system Si_3N_4-SiO_2-Y_2O_3-Al_2O_3 will have occurred by this temperature and although this appears not to inhibit the nitridation rate, it may have an undesirable impact upon grain growth of β-Si_3N_4 present in the nitrided microstructure. In subsequent experiments, a compromise temperature of 1370°C was used to maximise nitridation rate while retaining process control.

Full nitridation of all samples at 1370°C is accompanied by complete conversion of Si to Si_3N_4. However, the XRD traces for all compositions (series A and B) show a substantial level of β-Si_3N_4 even at this relatively early stage in the process chemistry. In fully nitrided samples the XRD ratio of $\beta(210)$: $[\beta(210) + \alpha(201)]$ exceeds 0·75. One reason for this might be seeding of the β phases, as β', due to minor amounts of Al. Guinier XRD unit cell measurements show little deviation from regular β-Si_3N_4 values, even for compositions 3 and 4, which have the highest Al_2O_3 content. It is interesting to compare this relatively high conversion to β-Si_3N_4 with the results achieved during nitridation of NPS-Si_3N_4 in which β:$(\beta + \alpha)$ values of 0·25 are more usual.[14] The XRD data of Fig. 3 show that there is no change in the α-Si_3N_4 level between pre-nitridation and full nitridation, whereas β-Si_3N_4, which was absent after pre-nitridation, has now become the dominant phase. The implication is that both the original added α-Si_3N_4 and the α-Si_3N_4 which forms at the pre-nitridation stage are slow to convert to β-Si_3N_4. However, the Si that is nitrided at higher temperatures is either converted to a 'reactive' form of α-Si_3N_4 which converts very

rapidly to β-Si_3N_4 or may even be converted directly to β-Si_3N_4. As noted above, there is very likely to be sufficient liquid phase present in this system at 1370°C to accelerate any solution-precipitation conversion of α-Si_3N_4 to β-Si_3N_4.[4,15] Also, this liquid becomes rapidly over saturated with nitrogen due to the continuous nitride formation and this will favour nucleation of the β phase. Small quantities of O'-sialon (Si_2N_2O) are present in all fully nitrided samples.

Considering now the alumina-containing phases, some α-Al_2O_3 is converted to $Y_3Al_5O_{12}$ (YAG) during nitridation, the quantity increasing with increasing alumina substitution in the sialon composition. Figure 6 shows the phase development in series A samples nitrided at 1370°C for 6 and 12 h. It is clear that YAG is an important phase in the nitridation chemistry of these sialon compositions. By extrapolation back to very low alumina levels, such as those used in NPS Si_3N_4 preparation, we may infer that YAG formation is also possible when Al_2O_3 is added only as a sintering aid at the 2% level. Under some circumstances, this might have a negative influence by competing for the Y_2O_3, which would then have reduced availability for removal of the silicon oxide and oxynitride film on the particles. However, under the conditions used in this study the reaction between Y_2O_3 and silicon oxides is complete at the pre-nitridation stage and YAG is not observed until the full nitridation temperature is achieved. On the basis that Y_2O_3 and some Al_2O_3 are likely to be present in a liquid phase at the 1370°C nitridation temperature, the formation of YAG may well take place by a reprecipitation or crystallisation process. Optionally, as some of the Al_2O_3 remains present as discrete particles both during and after nitridation, the YAG formation may result from solution (Y_2O_3)-solid (Al_2O_3) reaction processes. This issue is addressed again in
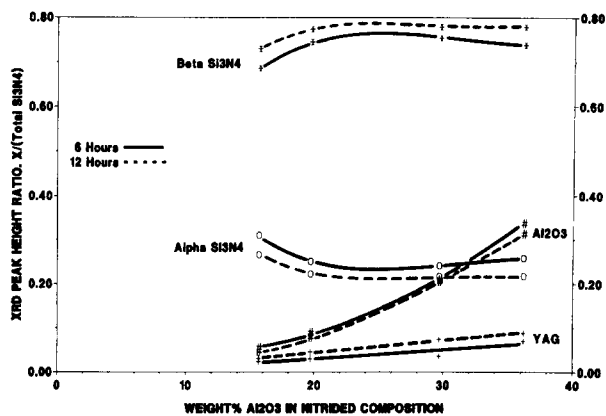

Fig. 6. Phase development during NPS sialon nitridation: effects of composition and time.

Section 3.3. Figure 6 shows that YAG increases with increasing Al_2O_3 content and this probably provides the only significant mechanism for Al_2O_3 reaction at these temperatures. The yttrium silicate phases present after the pre-nitridation step are totally consumed upon full nitridation in favour of a partial Si_3N_4-SiO_2-Y_2O_3-Al_2O_3 liquid phase[12] and YAG formation.

Nitridation of series B test bars (high surface areas) in the graphite resistance furnace showed consistency with the TGA results, all compositions could be fully nitrided in less than four hours at 1370°C. This compared favourably with previous results for NPS Si_3N_4[1] in which nitridation times of less than 3 h at 1350°C are normal. The reaction intermediates and products are the same as those for series A, i.e. early reaction of Y_2O_3 to form yttrium silicate phases and the progressive formation of YAG. Nitrided densities were in the range 67% (1B) to 74% (4B) theoretical. Linear shrinkage on nitridation ranged from 2·7% (1B) to 5·5% (4B), the higher shrinkage of series B reflecting their lower green densities when compared to series A samples. For fully nitrided series A samples, the densities were in the range 70–73% of theoretical and linear shrinkage ranged from 1% (composition 1A) to 3% (composition 4A).

3.2 Sintering behaviour

Figure 7 shows the densities obtained for compositions 1A–4A and 1B after 3 h sintering at temperatures in the range 1500–1830°C. For all compositions, the maximum density is achieved at relatively low temperatures (1575–1600°C) and for compositions 1 and 2 this density level is maintained throughout the entire test sequence, declining slightly at 1830°C. However, compositions 3 and 4 drop steadily in density immediately after achieving this maximum. In fact, specimens of these higher
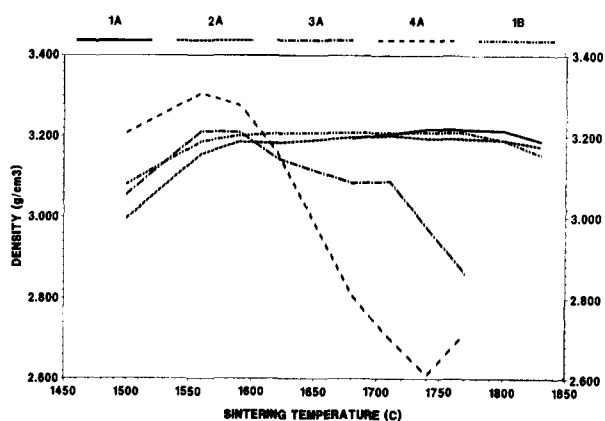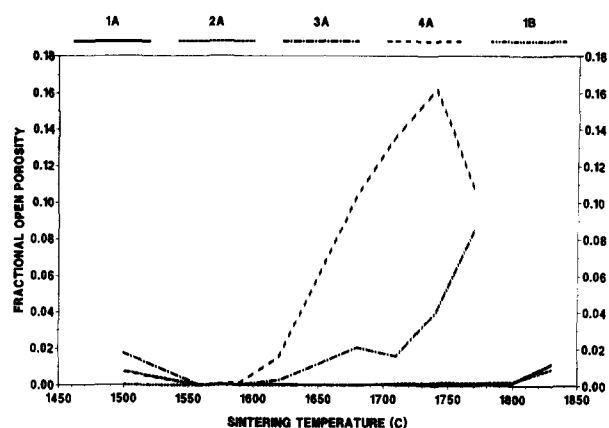

Fig. 8. Open porosity as a function of sintering temperature for NPS sialons.

alumina compositions show substantial bloating when heated much above 1600°C. These trends are reiterated in Fig. 8, which shows open porosity as a function of temperature for the same test specimens. The open porosities for all samples heated to 1575°C are less than 0·1%. For compositions 1 and 2, this is unchanged at 1675°C and rises only very slightly up to 1800°C. However, for compositions 3 and 4 the open porosities are 2% and 11%, respectively, by 1675°C, and much more above this temperature (Fig. 8).

The weight loss on sintering at 1575°C is 0·5–0·7% for all samples (Fig. 9). For compositions 1 and 2, this rises only slightly to 0·7–0·8% by 1675°C, but above 1800°C the weight losses exceed 2%. For compositions 3 and 4, the rate of weight loss increases markedly above 1650°C, reaching a maximum rate of loss at 1740°C. To a much reduced extent, this maximum loss at 1740°C may even be seen for composition 2, but there is no corresponding irregularity in the density or porosity (see Figs 7 and 8).
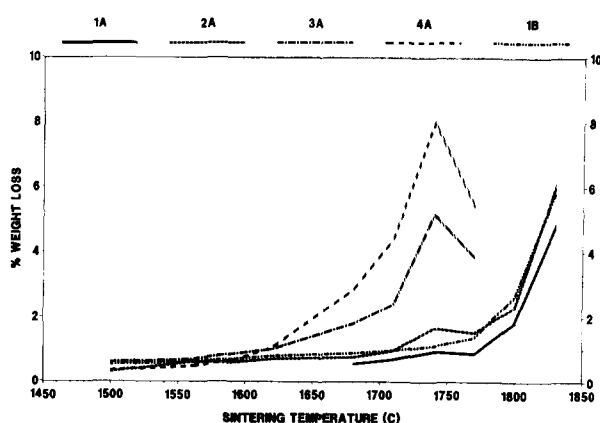
XRD shows that, for compositions 1 and 2

Fig. 7. Density as a function of sintering temperature for NPS sialons.

Fig. 9. Weight loss as a function of sintering temperature for NPS sialons.

Table 3. Unit cell versus z-values for β'-sialons sintered at 1775°C

Com-position	% Al_2O_3 in com-position	a ($\mathring{A}$)	c ($\mathring{A}$)	z (equi-valent)	z (XRD)
1	15·7	7·627 3 (5)	2·926 7 (3)	0·72	0·72
2	19·7	7·633 3 (6)	2·930 1 (6)	0·92	0·90
3	29·7	7·646 7 (6)	2·945 9 (7)	1·44	1·47
4	36·2	7·659 7 (10)	2·954 5 (8)	1·80	1·89

sintered to maximum density (1575°C and above), the only crystalline phase present is β'-sialon. Compositions 3 and 4 show significant free Al_2O_3 at 1575°C even though the samples have achieved their maximum density. The implication is that the rate controlling step in the alumina take-up is the ability of the sialon structure to incorporate the Al at 1575°C, rather than any problems due to alumina particle size. Between compositions 2 and 3 (that is, between 19·7 and 29·7 %wt Al_2O_3) there is a change in the solubility behaviour of alumina in these materials at 1575°C. This may be more clearly understood by reference to Fig. 1 in which it may be seen that above 19·7 %wt Al_2O_3 (composition 2) the sialon compositions move out from the β'–O' field defined by Jack[8] towards the β'-X-phase field. A detailed examination using the Guinier XRD technique was carried out in order to measure accurate unit cell values for β'-sialons sintered at 1775°C. The X-ray patterns were recorded on film using NBS Si powder as an internal standard. The films were interpreted by an automated optical recording system linked to a computing system that performed the unit cell refinement. Table 3 summarises these data and relates the observed β'-sialon unit cell to the degree of aluminium substitution, z, using the data of Haviar and Johannesen.[16] We may express each of the sialon compositions 1–4 used in this study in terms of an equivalent z-value, obtained by translation of the starting composition (parallel to the Si_3N_4–Si_3O_6 axis) from the Si_3N_4–Al_2O_3 join down on to the β'-sialon line on the sialon behaviour diagram. Within the error limits implicit in both the measurement and the unit cell-to-z conversion ($\approx 0·05$ in z), it can be seen that each composition has formed a β'-sialon whose Al content is very close to that predicted from the starting compositions. This evidence suggests that the β'-sialon phase formed on sintering remains stable in spite of the obvious bloating of the test specimens at high sintering temperatures as reflected in the density, porosity and weight loss in Figs 7–9. Consequently, the intergranular glassy phase is responsible for this decomposition, which, due to the redox nature of

reaction (5) below, results from loss of both nitrogen and SiO from the glass.
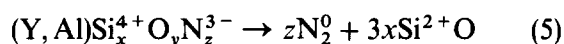
$$(Y, Al)Si_x^{4+}O_yN_z^{3-} \rightarrow zN_2^0 + 3xSi^{2+}O \qquad (5)$$

Figure 9 shows that this loss may reach 5 %wt and 8 %wt for compositions 3 and 4, respectively. Similar phenomena have been observed by Pugh *et al.*[17] for sialon compositions with high additive contents.

It is usually considered that α-Si_3N_4 is the preferred form of silicon nitride prior to sintering and that β-Si_3N_4 is not favourable to the densification process.[18] In the present case, however, full densities are achieved at relatively low temperatures with no obvious difficulty. There are two reasons for this. First, the β phase present in the nitrided materials must be converted to β' in the sintered materials, which usually proceeds via a solution-precipitation mechanism. This process may well be accelerated by a 'seeding' effect from the submicron β-Si_3N_4, which may therefore have an active rather than inhibitive role in the densification mechanism. Such a seeding effect has been reported previously for both α'- and β'-sialons.[19] Secondly, the high powder surface area and hence fast nitridation time generates nano-sized β-Si_3N_4, which has a high solubility in the grain boundary liquid, whereas in conventional processing the β phase is slow to dissolve, principally because relatively coarse β-containing powders are commonly used. In the present work, the fast dissolution-reprecipitation processes manifest themselves in terms of a very fine-grained microstructure (0·1–0·2 μm) at low sintering temperatures, as described elsewhere.[20]

3.3 The effect of Y_2O_3 addition level

Test bars of composition 2 were also prepared with 3% added Y_2O_3, instead of 6%, as described earlier. There is a clear impact on the nitridation chemistry which is already apparent at the pre-nitridation stage. In common with the standard 6% Y_2O_3 conditions, all Y_2O_3 is consumed during the pre-nitridation step. However, the extent of the weight gain achieved during this 1200°C step is substantially reduced to $\approx 1\%$, compared to more normal values of 10–16% for 6% Y_2O_3 specimens (see Section 3.1). This means that there has been insufficient Y_2O_3 added to fully react with the surface silicon oxide/oxynitride on the Si particles, inhibiting nitrogen access to the silicon surface. A further indication that this may be the case is the reduced level of yttrium silicate phases apparent in XRD traces of pre-nitrided specimens. For example, the major reflection for α-$Y_2Si_2O_7$ ($d = 3·01 \mathring{A}$) is

reduced to 0·42 of the 6% Y_2O_3 level following pre-nitridation, for XRD peaks of comparable peak-width and hence comparable crystallinity.

Experiments in which the nitridation schedule was curtailed after 25, 50 and 75% of the time for complete nitridation were carried out so as to follow the process chemistry in more detail. After 25% nitridation time all α-$Y_2Si_2O_7$ in both 3% and 6% specimens is consumed and simultaneously the alumina levels, which were identical in both specimens, drop to 60% of their former value. However, no new crystalline alumina- or yttria-containing phases are apparent. This is fully consistent with the TDA observation of liquid phase formation as low as 1300°C. After 50% nitridation time, YAG XRD peaks are well developed in the 6% specimens but no YAG is seen in the 3% specimens. Between 50 and 100% nitridation time, the trend is similar to that shown in Fig. 6, i.e. for the standard 6% Y_2O_3 specimens there is a slow increase in YAG with time at 1370°C. However, the 3% specimens remain free of YAG. We observe that the free alumina levels in both 3% and 6% specimens *remain identical to one another* during this latter part of the nitridation schedule. This implies that the YAG is sourced primarily from the liquid phase formed during the nitridation process and not from reaction of yttria-rich phases with free alumina particles. With respect to silicon-containing phases, Si_2N_2O (which was absent after pre-nitridation), increases continuously throughout the nitridation process in both 3% and 6% specimens but with 50–100% increased levels in the 3% specimens. It appears that low alumina levels in the early-formed glass phase encourages greater crystallisation of Si_2N_2O from the glass. Conversely, alumina may be considered to stabilise the glass phase at the 1370°C nitridation temperature, presumably by lowering the eutectic melting temperature. The impact of Y_2O_3 upon the α/β-Si_3N_4 ratio in the nitrided specimens is negligible, with a marginal decline in $\beta/(\beta + \alpha)$ from 0·79 (6%) to 0·76 (3%).

The effect of yttria addition on the sintering behaviour of NPS sialons is quite predictable and concurs with the known role of Y_2O_3 as a sintering aid. Sialon composition 2 with 3% added Y_2O_3 achieved its maximum density at $\approx 1675°C$, that is some 75° higher than for the 6% Y_2O_3 materials.

In summary, Y_2O_3 addition can be used as a very sensitive tool to control process chemistry particularly by its role in accelerating the nitridation chemistry. A balance must be sought which will allow maximum nitridation rate at the lowest temperature but not so as to form too much early

liquid, which may tend to close down the pore structure too soon and thus inhibit the nitridation. This factor is particularly important if specimen green densities are allowed to exceed $\approx 60\%$ of theoretical. For composition 2 sialons, the level of Y_2O_3 addition should optimally be greater than 3% but less than 6%.

4 Conclusions

This paper has demonstrated the applicability of the nitrided pressureless sintering technique to low alumina sialon compositions. The important features of NPS sialon processing are as follows:

(1) The nitridation rate is critically dependent on control of the milling conditions.

(2) Nitridation times under 3 h are achievable if powder surface areas are of the order of $20\ m^2\ g^{-1}$ and green densities prior to nitridation are kept no higher than 60% of theoretical.

(3) Sintered bodies achieve maximum density at relatively low temperatures, typically 1575–1600°C, starting with nitrided specimens of high $\beta/\alpha + \beta$ ratio, typically 0·75 and higher.

(4) There is a significant difference in sintering behaviour between the compositions corresponding to the extended β'-O' and β'-X-phase regions, the latter compositions showing a narrow firing range.

(5) Y_2O_3 added to assist the densification process also has a vital role in the early nitridation chemistry of these materials. YAG formation occurs during the second stage of the nitridation and hence does not obstruct the role of Y_2O_3 to remove the SiO_2/Si_2N_2O film from the Si particles during the first stage (pre-nitridation) step. 3% Y_2O_3 is insufficient to fulfil this function in the present system.

Our understanding of the process chemistry in these materials has enabled us to demonstrate that the NPS technique can be used to exercise a high degree of process control in sialon fabrication, leading to valuable economies such as Si for Si_3N_4 substitution and reduced firing times and temperatures. In future publications we shall present studies of the crystallisation behaviour of the intergranular glassy phase in these materials and the impact of this on the microstructure and mechanical properties of NPS sialons.[20]

Acknowledgements

References

1. Pompe, R., Hermansson, L. & Carlsson, R., Development of commercially advantageous techniques for fabrication of low shrinkage Si_3N_4-based materials. *Sprechsaal*, **115** (1982) 1098–101.
2. Pompe, R., SE 8103269-0 (1981), US 463,884 (1983), EP 82-00161 (1982).
3. Nyberg, B., Falk, L. K. L., Pompe, R. & Carlsson, R., Some features of nitrided pressureless sintered (NPS) silicon nitride materials made by modified preparation routes. In *Ceramic Materials and Components for Engines, Proc 2nd Int. Symp., Lubeck, 1986*, ed. W. Bunk & H. Hausner. Verlag Deutsche Keramische Gesellschaft,Berlin 1986, pp. 155–63.
4. Lewis, M. H., Powell, B. D., Drew, P., Lumby, R. J., North, B. & Taylor, A. J., The formation of single phase silicon-aluminium-oxygen-nitrogen ceramics. *J. Mater. Sci.*, **12** (1977) 61–74.
5. Thompson, D. P., Sun, W. Y. & Walls, P. A., O'-β' and α'-β' sialon ceramics. In *Ceramic Materials and Components for Engines, Proc. 2nd Int. Symp., Lubeck, 1986*, ed. W. Bunk & H., Hausner. Verlag Deutsche Keramische Gesellschaft, Berlin, 1986, pp. 643–50.
6. Gillot, L., Cowlam, N. & Bacon, G. E., A neutron diffraction investigation of some β'-sialons. *J, Mater. Sci.*, **16** (1981) 2263–8.
7. Brown, I. W. M., Pompe, R. & Carlsson, R., Preparation of sialons by the NPS technique, Presented at the 1st European Ceramic Society Conf., Maastricht, The Netherlands, 1989. In *Euro-Ceramics Volume I (Processing of Ceramics)*, ed. G. de With, R. A. Terpstra & R. Metselaar, Elsevier Applied Science, London, 1989, pp. 1.484–1.488.
8. Jack, K. H., Sialons and related nitrogen ceramics. *J. Mater. Sci.*, **11** (1976) 1135–58.
9. Trigg, M. B. & Jack, K. H., Solubility of aluminium in silicon oxynitride. *J. Mater. Sci. Letts.*, **6** (1987) 407–8.
10. Johnsson, A., Carlström, E., Hermansson, L. & Carlsson, R., Rate-controlled extraction unit for removal of organic binders from injection-moulded ceramics. In *Ceramic Powders*, ed. P. Vincenzini. Elsevier, Amsterdam, 1983, pp. 767–72.
11. Pompe, R., Hermansson, L., Johansson, T., Djurle, E. & Hatcher, M. E., Characterisation of silicon powders for the production of Si_3N_4. *Mater. Sci. Eng.*, **71** (1985) 355–62.
12. O'Meara, C., Dunlop, G. L. & Pompe, R., Formation, crystallisation and oxidation of selected glasses in the Y-Si-Al-O-N system. *J. Mater. Sci.* (1990) (in press).
13. Bergström, L. & Pugh, R. J., Interfacial characterisation of silicon nitride powders. *J. Am. Ceram. Soc.*, **72** (1989) 103–9.
14. Falk, L. K. L., Pompe, R. & Dunlop, G. L., Development of microstructure during nitridation and sintering of $Si:Si_3N_4$ powder compacts. In *Science of Ceramics 12*, ed. P. Vincenzini. Ceramurgia s.r.l., Faenza, Italy, 1984, pp. 293–8.
15. Morgan, P. E. D., The α/β-Si_3N_4 question. *J. Mater. Sci. Letts.*, **15** (1980) 791–3.
16. Haviar, M. & Johannesen, O., Unit-cell dimensions of β'-sialons. *Adv. Ceram. Mater.*, **3** (1988) 405–7.
17. Pugh, M. D., Zarnon, L. & Drew, R. A. L., Controlled processing of β'-sialons containing Y_2O_3 additions. In *Ceramic Transactions, Vol. 1: Ceramic Powder Science*, ed. G. L. Messing, E. R. Fuller & H. Hausner. American Ceramic Society, Westonville, Ohio, 1988, pp. 1051–8.
18. Ekström, T., Ingelström, N., Brage, R., Hatcher, M. & Johansson, T., α-β sialon ceramics made from different silicon nitride powders. *J. Amer. Ceram. Soc.*, **71** (1988) 1164–70.
19. Chatfield, C., Ekström, T. & Mikus, M., Microstructural investigation of alpha-beta yttrium sialon materials. *J. Mater. Sci.*, **21** (1986) 2297–307.
20. Brown, I. W. M., O'Meara, C. & Pompe, R., Microstructure of NPS sialons. In preparation.